

Research Article
Periodontal Science



Differential gene expression profiles of periodontal soft tissue from rat teeth after immediate and delayed replantation: a pilot study

Yong Kwon Chae ^{1,2,*}, Seo Young Shin ^{2,*}, Sang Wook Kang ³,
Sung Chul Choi ¹, Ok Hyung Nam ^{1,*}

¹Department of Pediatric Dentistry, School of Dentistry, Kyung Hee University, Seoul, Korea

²Department of Dentistry, Graduate School, Kyung Hee University, Seoul, Korea

³Department of Oral and Maxillofacial Pathology, School of Dentistry, Kyung Hee University, Seoul, Korea



Received: Aug 13, 2021

Revised: Sep 27, 2021

Accepted: Nov 3, 2021

Published online: Nov 26, 2021

***Correspondence:**

Ok Hyung Nam

Department of Pediatric Dentistry, Kyung Hee University School of Dentistry, 26 Kyungheedaero, Dongdaemun-gu, Seoul 02447, Korea.

Email: pedokhyung@gmail.com

Tel: +82-2-958-9371

Fax: +82-2-958-9478

^{*}Yong Kwon Chae and Seo Young Shin contributed equally as first authors.

Copyright © 2022. Korean Academy of Periodontology

This is an Open Access article distributed under the terms of the Creative Commons Attribution Non-Commercial License (<https://creativecommons.org/licenses/by-nc/4.0/>).

ORCID iDs

Yong Kwon Chae

<https://orcid.org/0000-0001-8059-9305>

Seo Young Shin

<https://orcid.org/0000-0002-3651-9635>

Sang Wook Kang

<https://orcid.org/0000-0002-0358-2304>

Sung Chul Choi

<https://orcid.org/0000-0001-7221-2000>

Ok Hyung Nam

<https://orcid.org/0000-0002-6386-803X>

ABSTRACT

Purpose: In dental avulsion, delayed replantation usually has an uncertain prognosis. After tooth replantation, complex inflammatory responses promote a return to periodontal tissue homeostasis. Various types of cytokines are produced in the inflammatory microenvironment, and these cytokines determine the periodontal tissue response. This study aimed to identify the gene expression profiles of replanted teeth and evaluate the functional differences between immediate and delayed replantation.

Methods: Maxillary molars from Sprague-Dawley rats were extracted, exposed to a dry environment, and then replanted. The animals were divided into 2 groups according to the extra-oral time: immediate replantation (dry for 5 minutes) and delayed replantation (dry for 60 minutes). Either 3 or 7 days after replantation, the animals were sacrificed. Periodontal soft tissues were harvested for mRNA sequencing. Hallmark gene set enrichment analysis was performed to predict the function of gene-gene interactions. The normalized enrichment score (NES) was calculated to determine functional differences.

Results: The hallmark gene sets enriched in delayed replantation at 3 days were oxidative phosphorylation (NES=2.82, $Q<0.001$) and tumor necrosis factor-alpha (TNF- α) signaling via the nuclear factor kappa light chain enhancer of activated B cells (NF- κ B) pathway (NES=1.52, $Q=0.034$). At 7 days after delayed replantation, TNF- α signaling via the NF- κ B pathway (NES=-1.82, $Q=0.002$), angiogenesis (NES=-1.66, $Q=0.01$), and the transforming growth factor-beta signaling pathway (NES=-1.46, $Q=0.051$) were negatively highlighted.

Conclusions: Differentially expressed gene profiles were significantly different between immediate and delayed replantation. TNF- α signaling via the NF- κ B pathway was marked during the healing process. However, the enrichment score of this pathway changed in a time-dependent manner between immediate and delayed replantation.

Keywords: Gene expression profiling; RNA sequencing; Tooth avulsion; Tooth replantation

Funding

This work was supported by the National Research Foundation of Korea (NRF) grant funded by the Korea government (MSIT) (No. 2020R1C1C1006937).

Author Contributions

Conceptualization: Ok Hyung Nam; Formal analysis: Yong Kwon Chae, Sung Chul Choi; Investigation: Yong Kwon Chae, Seo Young Shin, Ok Hyung Nam; Methodology: Sang Wook Kang, Sung Chul Choi, Ok Hyung Nam; Project administration: Ok Hyung Nam; Writing - original draft: Yong Kwon Chae, Ok Hyung Nam; Writing - review & editing: Sang Wook Kang, Ok Hyung Nam.

Conflict of Interest

No potential conflict of interest relevant to this article was reported.

INTRODUCTION

Periodontal tissues respond to various stimuli to maintain homeostasis via ecological interactions between the host and the stimulus. Disruption of the ecological balance affects the restoration of periodontal tissue homeostasis, resulting in periodontal disease progression [1]. Oral bacteria are associated with periodontal disease and trigger immune responses in periodontal tissues [2]. The innate immune response, an initial inflammatory process, is a physiologic defense mechanism against periodontal pathogens. Chronic inflammation induces an adaptive immune response. Overactivation of the immune response induces osteoclastic activity and leads to periodontal complications such as alveolar bone loss. Thus, disease susceptibility depends on the net effect of innate and adaptive immune responses [3]. A similar phenomenon can be observed in periodontal tissue responses after replantation of avulsed teeth [4]. After replantation, an immune response is evoked to protect the periradicular tissues before wound healing. Moreover, an immune response is activated during healing if bacteria invade the periodontal ligament (PDL) space [5]. Thus, the fate of replanted teeth is determined by the competition between cellular responses and bacterial invasion [4].

Severe periodontal damage in avulsion injuries may lead to inflammatory or replacement root resorption after replantation. The extra-oral time is a clinically critical factor associated with the development of root resorption [6]. Previous studies have demonstrated that the incidence of root resorption increased in replanted teeth with an extra-oral time greater than 5 minutes [7]. A prolonged extra-oral time affects the viability of the PDL [6]. There is a consensus that PDL cell survival is impossible if the extra-oral time exceeds 60 minutes. Thus, periodontal tissue degeneration and apoptosis are more likely to occur with prolonged extra-oral time [8].

Cytokines determine the periodontal tissue response after replantation of avulsed teeth by modulating host immune mechanisms. Cytokine-cytokine interactions construct networks that activate signaling transduction pathways and regulate the host response against periodontal pathogens [3]. A previous study demonstrated that a prolonged extra-oral time of replanted teeth was correlated with the expression of pro-inflammatory cytokines, including tumor necrosis factor-alpha (TNF- α), interleukin (IL)-6, and IL-1 β [9]. Another study demonstrated highlighted expression of osteoprotegerin, receptor activator of nuclear factor κ B (RANK), and RANK ligand (RANKL) in immediately replanted rat teeth in the initial period of up to 3 days [10]. However, the biological function of cytokine-cytokine interactions after replantation has not been fully identified. Therefore, a comprehensive understanding of cytokine-cytokine interactions is necessary to detect changes after tooth replantation.

Previous studies have investigated gene expression profiles in periodontitis-affected gingival tissues to identify the pathogenesis of periodontitis using DNA microarrays [11,12]. RNA-sequencing (RNA-seq), a high-throughput sequencing technology, provides more accurate and sensitive measurements in gene screening and quantification than DNA microarrays. Moreover, bioinformatics analyses of RNA-seq data can precisely identify changes in tissue-derived gene expression profiles and biologic pathways from gene networks [13]. Evaluating changes in gene expression profiles and related biologic pathways can provide a better understanding of dynamic periodontal tissue responses in replanted teeth. Therefore, the purpose of the present study was to identify gene expression profiles after tooth replantation by RNA-seq and to evaluate the functional information generated by gene-gene networks in immediate replantation (IR) and delayed replantation (DR).

MATERIALS AND METHODS

Animal group allocation

The experimental protocol was reviewed and approved by the Ethics in Institutional Animal Care and Use Committee of Kyung Hee Medical Center, Kyung Hee University, Seoul, Korea (KHMC-IACUC-20-012). This study was designed in accordance with the ARRIVE guideline. Thirteen healthy male Sprague-Dawley rats (age: 4–6 weeks; weight: 150–200 g) were purchased from KOATECH (Pyeongtaek, Korea). This study used a split-mouth design. Twelve rats underwent extraction of their 24 bilateral first molars, while 1 remaining rat did not receive any extraction. Its maxillary first molar was used as the control group. The 24 molars were then randomly assigned into 2 sets of experimental groups (IR and DR) according to the extra-oral dry time. The molars in the IR groups were replanted after 5 minutes of dry storage and those of DR groups after 60 minutes of dry storage. There were 4 experimental groups according to whether the molars underwent IR or DR and the time of sacrifice.

- i) IR3: IR group sacrificed at 3 days after replantation (n=6)
- ii) IR7: IR group sacrificed at 7 days after replantation (n=6)
- iii) DR3: DR group sacrificed at 3 days after replantation (n=6)
- iv) DR7: DR group sacrificed at 7 days after replantation (n=6)
- v) Control: no extraction (n=1)

Experimental procedures

The animals received a 5-day supply of 0.4% β -aminopropionitrile (Sigma-Aldrich, St Louis, MO, USA) with a powdered Purina rat diet to minimize trauma during extraction. The animals were anesthetized with an intraperitoneal injection of 30 mg/kg tiletamine hydrochloride and zolazepam (Zoletil 50; Virbac Lab, Carros, France). As a complementary local anesthetic, 2% lidocaine with 1:80,000 epinephrine (Lignospan; Septodont, Saint-Maur-des-Fossés, France) was administered. After cleaning the oral cavity with 2% chlorhexidine solution, bilateral extraction of the maxillary first molars was performed gently using sterile dressing tissue forceps. After excluding any roots that were fractured during extraction, the allotment of 6 teeth per group was maintained by including additional experimental animals. The extracted molars were exposed to a dry environment for 5 or 60 minutes at room temperature.

Before replantation, only molars with DR received endodontic treatment to minimize inflammatory root resorption associated with pulp necrosis. After creating an endodontic access, the pulp tissue was extirpated, and the root canals were prepared using a sterile #15 K-file (Dentsply Maillefer, Tulsa, OK, USA). We used 2% sodium hypochlorite and saline for canal disinfection. The canal was filled with calcium hydroxide/iodoform paste (Vitapex; Neodental, Tokyo, Japan), and a composite resin (3M ESPE Filtek Z250; 3M ESPE, St Paul, MN, USA) was used to seal the access. The root surfaces and alveolar sockets were cleaned with saline before replantation. After replantation, all animals received a single intramuscular injection of 20,000 IU of penicillin G (Alvogen potassium penicillin G, Alvogen, Seoul, Korea) and were fed a powdered Purina rat diet for 3 or 7 days. On the sacrifice day, anesthesia was achieved with an intramuscular injection of Zoletil 50 (100 mg/kg). Periodontal soft tissue from the sulcus to the palatal attached gingiva of the molars was collected using sterile #15 blades. The tissue samples were flash-frozen in liquid nitrogen and transferred for RNA-seq.

RNA-seq procedure and identification of differentially expressed genes (DEGs)

The RNA-seq procedure was performed as previously described [14,15]. Briefly, 5 µg of total RNA for each sample was isolated. RNA quality was assessed using the Agilent 2100 bioanalyzer with the RNA 6000 Nano Chip (Agilent Technologies). The quality assessment was conducted using the RNA integrity number (RIN), and it was confirmed that all samples showed RIN values greater than 6. RNA libraries were constructed using a QuantSeq 3' mRNA-Seq Library Prep Kit (Lexogen Inc., Vienna, Austria). The library was amplified to add the complete adapter sequences required for cluster generation. The finished library was purified from polymerase chain reaction (PCR) components. High-throughput sequencing was performed on single-read 75 bp fragments using a NextSeq 500 (Illumina Inc., San Diego, CA, USA). Differential gene expression was then determined based on the read count using coverage in BEDtools [16]. DEGs were identified using the ExDEGA 2.5.0 program (EBIOGEN, Seoul, Korea) as genes with more than 2-fold differences in expression relative to the control. The Database for Annotation, Visualization, and Integrated Discovery (DAVID v 6.8) (<http://david.abcc.ncifcrf.gov>) was used to search for the classification of DEGs. All relevant mRNA-seq data were deposited in GEO (No. GSE173622).

Validation of RNA-seq data using real-time PCR

Quantitative real-time PCR (qRT-PCR) was used to validate the RNA-seq data. Total RNA was isolated from some of the samples (n=4 per group). Briefly, 5 µg of total RNA was converted into complementary DNA (cDNA) by reverse transcriptase (SuperScript™ II Reverse Transcriptase; Invitrogen, Carlsbad, CA, USA). Next, a StepOnePlus Real-Time PCR system was used to measure SYBR green fluorescence with a commercial reagent (Power SYBR Green Master Mix; Thermo Fisher Scientific, Carlsbad, CA, USA). The cycling conditions were as follows: denaturation for 10 minutes at 95°C, followed by 40 amplification cycles of denaturation for 10 s at 95°C, and annealing for 45 s at 59°C. The cDNA levels were normalized to GAPDH levels using the $2^{-\Delta\Delta Ct}$ method. The experiments were performed in triplicate. The primer sequences used for PCR were as follows: TNF- α , (F) 5'-GACCAGGCTGTCGCTACATC-3', (R) 5'-ACCCGTAGGGCGATTACAGT-3'; IL-6, (F) 5'-ATGAGGTCTACTCGGCAAAC-3', (R) 5'-CTGACCACAGTGAGGAATGTC-3'; IL-1 β , (F) 5'-GGCAGCATGTGTCGACAGAAG-3', (R) 5'-TGTGCACTGGTCCAAATTCA-3'; GAPDH, (F) 5'-ACAGTCAAGGCTGAGAATGG-3', (R) 5'-GATCTCGCTCCTGGAAGATG-3'.

Bioinformatics analysis

For predicting the functional profiles of gene-gene interaction networks, gene set enrichment analysis (GSEA) was performed on normalized data from each group utilizing an online GSEA program (<http://software.broadinstitute.org/gsea/index.jsp>) that uses gene sets based on the Molecular Signature Database (MSigDB v 7.2.). Kyoto Encyclopedia of Genes and Genomes (KEGG) enrichment analysis was used to obtain functional information on gene interaction networks.

To further identify the differences in functional profiles between IR and DR in a time-dependent manner, RNA-seq data of each sample were evaluated. Hallmark gene sets were generated using the GSEA v. 4.1.0. program. The DR and IR sets were each compared for sacrifice times of 3 and 7 days (DR3 vs. IR3 and DR7 vs. IR7). The relative power of gene sets between the groups was compared by enrichment plot analysis. Enrichment scores (ES) and normalized enrichment scores (NES) were generated.

To evaluate the interactions, we used the Search Tool for the Retrieval of Interacting Genes (STRING) database (<https://string-db.org/cgi/input.pl>) to construct protein-protein interaction (PPI) networks. The minimum required interaction score was set at a high confidence interval (>0.700), and the inflation parameter was set as 3 for MCL clustering.

Statistical analysis

In the DEG analysis, a *P*-value <0.05 was considered to indicate differential expression in genes. To assess KEGG enrichment pathways, only gene sets with false discovery rates (FDRs) corresponding to a *Q*-value <0.05 were included. To calculate ES and NES, nominal *P*-values were calculated. Gene sets with an FDR *Q*-value <0.25 and a nominal *P*-value <0.05 were considered statistically significant.

RESULTS

The clustering heatmap analysis demonstrated homogeneity of the samples in each group (Figure 1A). Principal component analysis showed differences in terms of genetic diversity

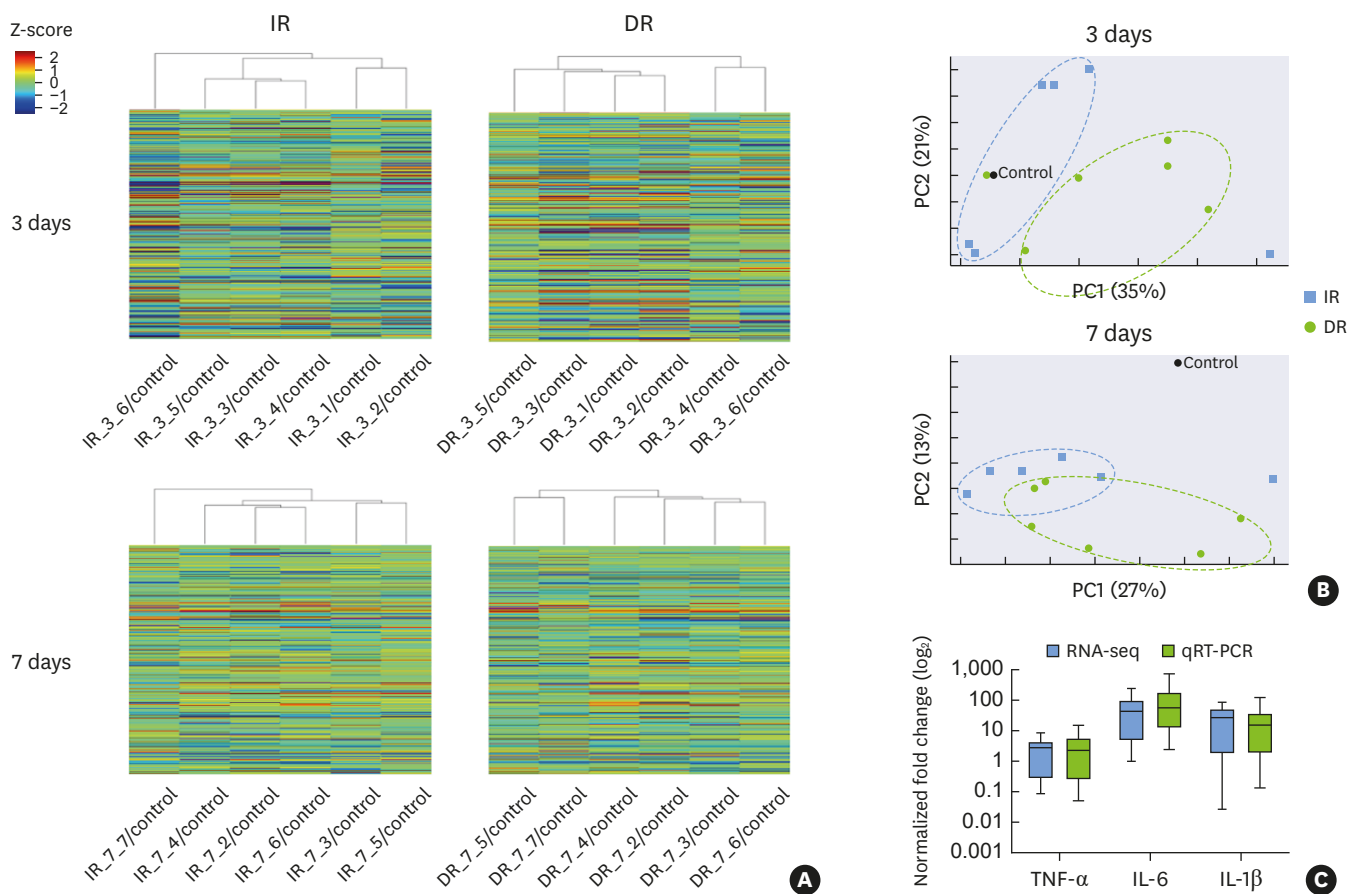
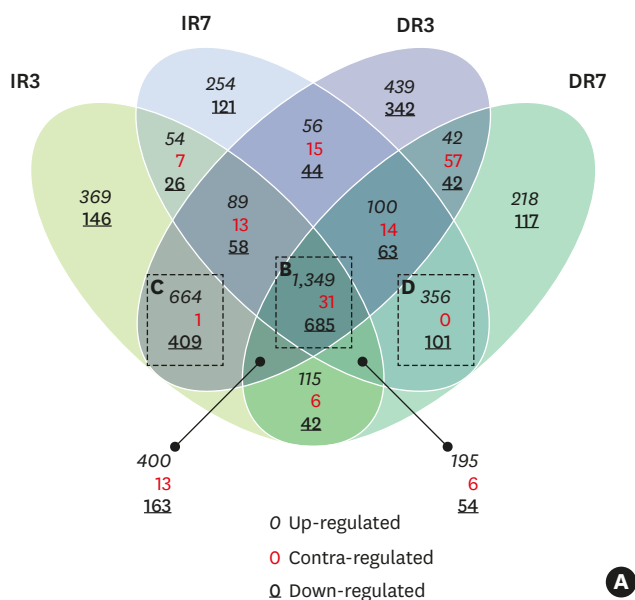


Figure 1. RNA-seq data after IR and DR. (A) Clustering heatmaps showing the homogeneity of gene expression profiles of the samples in each group. (B) Two-dimensional principal component analysis showing the diversity of samples. (C) RNA-seq data was confirmed by some of the RNA samples (n=4 in each group) by quantitative real-time polymerase chain reaction. The lines in the box plots represent the mean values of the samples.

IR: immediate replantation, DR: delayed replantation, IR3: 3 days after immediate replantation, DR3: 3 days after delayed replantation, IR7: 7 days after immediate replantation, DR7: 7 days after delayed replantation, RNA-seq: RNA-sequencing, qRT-PCR: quantitative real-time polymerase chain reaction, TNF- α : tumor necrosis factor-alpha, IL: interleukin.

among the experimental groups (**Figure 1B**). Three biological markers for periodontal disease activity (TNF- α , IL-6, and IL-1 β) were selected for qRT-PCR. The accuracy of RNA-seq data was confirmed by similar expression patterns of these genes between the RNA-seq analysis and qRT-PCR (**Figure 1C**).

A Venn diagram analysis of the 4 experimental groups compared to the control group revealed that 2065 DEGs (1,349 upregulated, 685 downregulated, and 31 contra-regulated) overlapped in all experimental groups (**Figure 2A**). Among the shared DEGs, cytokine-cytokine receptor interactions, the JAK-STAT signaling pathway, the chemokine signaling pathway, the mitogen-activated protein kinase (MAPK) signaling pathway, the Toll-like receptor signaling pathway, and transforming growth factor-beta (TGF- β) pathway were identified as enriched KEGG pathways (**Figure 2B**). Between IR3 and DR3, the peroxisome, TGF- β pathway, and PPAR signaling pathways were significantly enriched (**Figure 2C**). Cytokine-cytokine receptor interactions, the T-cell receptor signaling pathway, and the chemokine signaling pathway showed significant enrichment between IR7 and DR7 (**Figure 2D**). The top 10 DEGs that were upregulated and downregulated in the DR groups compared to the control are shown in **Figure 3**. Notably, CXCL2 expression in the DR groups was remarkably upregulated at both 3



KEGG pathway	Genes in overlap (n)	FDR Q value
Cytokine cytokine receptor interaction	151	8.28×10^{-228}
JAK-STAT signaling pathway	56	6.43×10^{-67}
Chemokine signaling pathway	47	2.72×10^{-47}
Melanoma	31	5.78×10^{-40}
Pathways in cancer	45	2.00×10^{-33}
MAPK signaling pathway	38	1.18×10^{-28}
Autoimmune thyroid disease	22	4.47×10^{-28}
Toll like receptor signaling pathway	27	4.51×10^{-28}
Cytosolic DNA sensing pathway	22	1.62×10^{-27}
TGF- β signaling pathway	24	1.19×10^{-25}

KEGG pathway	Genes in overlap (n)	FDR Q value
Valine leucine and isoleucine degradation	17	5.54×10^{-14}
Peroxisome	17	1.11×10^{-9}
Propanoate metabolism	11	2.22×10^{-8}
Biosynthesis of unsaturated fatty acids	8	1.72×10^{-6}
Glutathione metabolism	11	1.72×10^{-6}
Pyruvate metabolism	9	1.98×10^{-5}
FC- γ receptor mediated phagocytosis	13	3.00×10^{-5}
TGF- β signaling pathway	12	4.89×10^{-5}
PPAR signaling pathway	10	2.08×10^{-4}
Glycine serine and threonine metabolism	7	2.08×10^{-4}

KEGG pathway	Genes in overlap (n)	FDR Q value
Cytokine cytokine receptor interaction	21	2.25×10^{-10}
T cell receptor signaling pathway	14	9.10×10^{-10}
NK cell mediated cytotoxicity	15	1.31×10^{-9}
Cell adhesion molecules (CAMs)	14	7.85×10^{-9}
Asthma	8	2.57×10^{-8}
Chemokine signaling pathway	15	6.16×10^{-8}
Pathways in cancer	19	6.16×10^{-8}
Primary immunodeficiency	8	6.16×10^{-8}
Hematopoietic cell lineage	10	6.20×10^{-7}
Leishmania infection	9	1.32×10^{-6}

Figure 2. Overview of gene expression profiles. (A) Venn diagram analysis. (B-D) KEGG pathway analysis. The analysis was performed the expressed genes in the box with the corresponding uppercase letters in (A). Only sets with an FDR Q value < 0.05 were included. (B) The top 10 KEGG pathways significantly enriched in all experimental groups. (C) The top 10 KEGG pathways in the groups at 3 days. (D) The top 10 KEGG pathways in the groups at 7 days. IR3: 3 days after immediate replantation, IR7: 7 days after immediate replantation, DR3: 3 days after delayed replantation, DR7: 7 days after delayed replantation, KEGG: Kyoto Encyclopedia of Genes and Genomes, FDR: false discovery rate, MAPK: mitogen-activated protein kinase, TGF- β : transforming growth factor-beta.

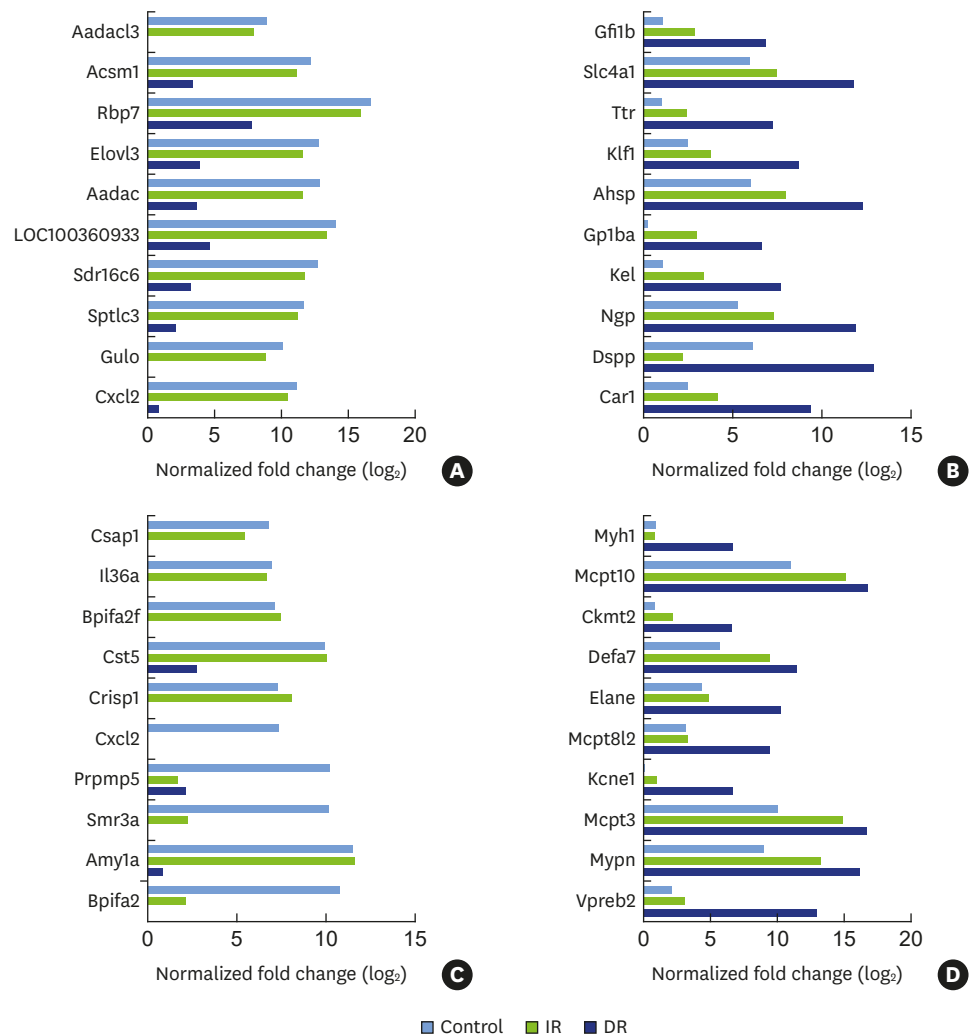


Figure 3. The top 10 DEGs upregulated or downregulated in IR and DR conditions. (A) The top 10 upregulated DEGs in the groups at 3 days. (B) The top 10 downregulated DEGs in the groups at 3 days. (C) The top 10 upregulated DEGs in the groups at 7 days. Note that CXCL2 expression in IR was similar to that in the control group. (D) The top 10 downregulated DEGs in the groups at 7 days. IR: immediate replantation, DR: delayed replantation, DEG: differentially expressed gene.

and 7 days, whereas in the IR groups, its expression was strongly upregulated only at 3 days and was similar to that of the control at 7 days.

Enrichment plot analysis was performed to investigate functional differences in identified DEGs between the IR and DR conditions in a time-dependent manner. The enriched biological functions mainly involved oxidative phosphorylation (NES=2.82, $Q < 0.001$), TNF- α signaling via the nuclear factor kappa light chain enhancer of activated B cells (NF- κ B) pathway (NES=1.52, $Q = 0.034$), and peroxisome (NES=1.42, $Q = 0.069$) in DR3 compared to IR3 (Table 1). The epithelial-mesenchymal transition (NES=-2.34, $Q < 0.001$), oxidative phosphorylation (NES=-1.90, $Q = 0.001$), TNF- α signaling via the NF- κ B pathway (NES=-1.82, $Q = 0.002$), angiogenesis (NES=-1.66, $Q = 0.01$), the TGF- β signaling pathway (NES=-1.46, $Q = 0.051$), and the IL-2 STAT5 signaling pathway (NES=-1.28, $Q = 0.202$) were negatively highlighted in DR7 compared to IR7 (Table 2). Enrichment plots of TNF- α signaling via the NF- κ B pathway revealed differences in DEGs with time. The pathway was positively correlated

Table 1. Hallmark gene sets significantly enriched in DR3 compared to IR3

Hallmark gene set	ES	NES	Nominal <i>P</i> value	FDR <i>Q</i> value
Oxidative phosphorylation	0.58	2.82	<0.001	<0.001
Myogenesis	0.50	2.42	<0.001	<0.001
Adipogenesis	0.47	2.29	<0.001	<0.001
Fatty acid metabolism	0.46	2.19	<0.001	<0.001
mTOR complex 1 (mTORC1) signaling	0.38	1.89	<0.001	<0.001
TNF- α signaling via NF- κ B	0.32	1.52	0.002	0.034
Peroxisome	0.32	1.42	0.012	0.069
Bile acid metabolism	0.31	1.39	0.031	0.084
IFN- α response	0.31	1.34	0.038	0.115

DR3: 3 days after delayed replantation, IR3: 3 days after immediate replantation, ES: enrichment score, NES: normalized enrichment score, FDR: false discovery rate, MTOR: mammalian target of rapamycin, TNF- α : tumor necrosis factor-alpha, NF- κ B: nuclear factor kappa light chain enhancer of activated B cells, IFN: interferon. Nominal *P* value <0.05; FDR *Q* value <0.25.

Table 2. Hallmark gene sets significantly enriched in DR7 compared to IR7

Hallmark gene set	ES	NES	Nominal <i>P</i> value	FDR <i>Q</i> value
Myogenesis	-0.58	-2.52	<0.001	<0.001
Epithelial-mesenchymal transition	-0.54	-2.34	<0.001	<0.001
Oxidative phosphorylation	-0.43	-1.90	<0.001	0.001
TNF- α signaling via NF- κ B	-0.41	-1.82	<0.001	0.002
Hypoxia	-0.39	-1.72	<0.001	0.006
Apical junction	-0.36	-1.55	<0.001	0.022
Coagulation	-0.38	-1.58	0.001	0.020
Angiogenesis	-0.50	-1.66	0.003	0.010
Complement	-0.34	-1.48	0.004	0.045
UV response up	-0.32	-1.37	0.024	0.107
TGF- β signaling	-0.41	-1.46	0.034	0.051
IL-2 STAT5 signaling	-0.29	-1.28	0.047	0.202

DR7: 7 days after delayed replantation, IR7: 7 days after immediate replantation, ES: enrichment score, NES: normalized enrichment score, TNF- α : tumor necrosis factor-alpha, NF- κ B: nuclear factor kappa light chain enhancer of activated B cells, UV: ultraviolet, TGF- β : transforming growth factor-beta, IL: interleukin. Nominal *P* value <0.05; FDR *Q* value <0.25.

with DR3 and negatively correlated with DR7 (**Figure 4A**). The profiles of the core enrichment genes were different with time (**Figure 4B**).

PPI network analysis was also performed to evaluate the regulatory mechanism of core enrichment genes with time. The network of DR3 presented significantly highlighted clustering, including STAT5A, CSF2, CXCL10, and NFIL3 (**Figure 5A**). The networks contained 45 nodes and 13 edges, and the PPI enrichment *P*-value was 1.8×10^{-6} . The network of DR7 presented 5 remarkable clusters, including IL6, FOS, and SERPINE1 (**Figure 5B**). The networks contained 94 nodes and 12 edges, and the PPI enrichment *P*-value was 2.96×10^{-11} .

DISCUSSION

In cases of avulsion injuries, IR is optimal to achieve successful tooth replantation. However, the replantation of avulsed teeth is often delayed due to insufficient knowledge about tooth replantation or low confidence among non-dental professionals [15]. Thus, current research regarding DR has focused on enhancing periodontal tissue healing with minimal complications. It is necessary to understand the biological differences in periodontal tissues between IR and DR in order to improve periodontal healing in replanted teeth.

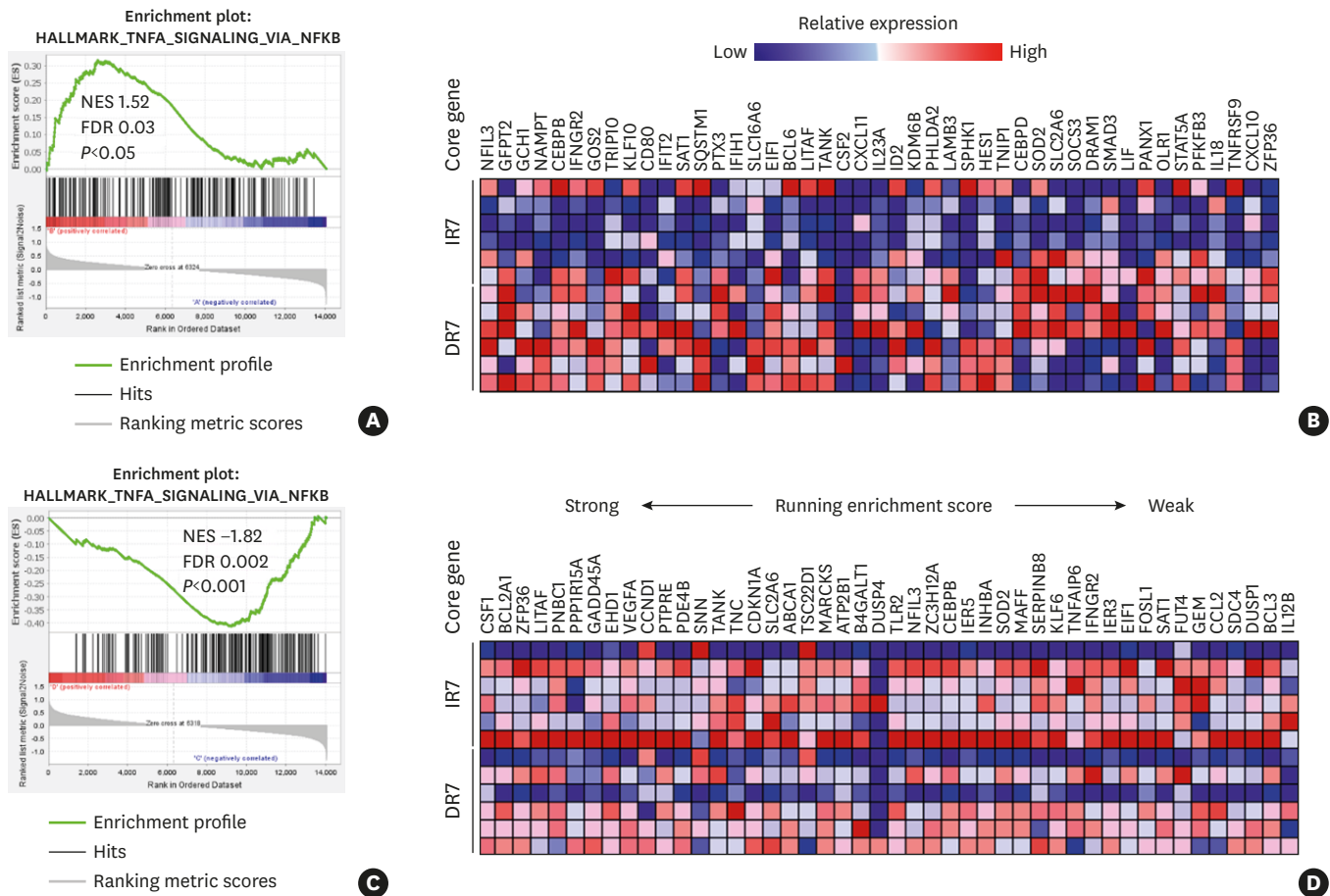


Figure 4. GSEA of TNF- α signaling via the NF- κ B pathway in delayed replantation. Enrichment plots and heatmaps for core enrichment genes were generated by the GSEA program v. 4.1.0 using hallmark gene sets. (A) Enrichment plot of DR3 versus IR3. The peak in the plot indicates upregulation of the gene sets associated with TNF- α signaling via the NF- κ B pathway in delayed replantation. (B) A heatmap for core enrichment genes. (C) Enrichment plot of DR7 versus IR7. The peak in the plot indicates downregulation of the gene sets associated with TNF- α signaling via the NF- κ B pathway in delayed replantation. (D) A heatmap of core enrichment genes. There was a difference in core enrichment genes between 3 and 7 days. NES: normalized enrichment score, FDR: false discovery rate, DR3: 3 days after delayed replantation, IR3: 3 days after immediate replantation, DR7: 7 days after delayed replantation, IR7: 7 days after immediate replantation, GSEA: gene set enrichment analysis, TNF- α : tumor necrosis factor-alpha, NF- κ B: nuclear factor kappa light chain enhancer of activated B cells.

In the present study, we compared the profiles of DEGs between IR and DR conditions. Next, KEGG enrichment analysis was performed to identify significantly highlighted pathways. The identified pathways confirmed that immune mechanisms against stimuli occurred primarily in replanted teeth. Toll-like receptor pathways are crucial for initiating the innate immune response [17]. The JAK-STAT signaling pathway upregulates IL-6 production and further integrates the MAPK signaling pathway [18]. IL-6 is a pro-inflammatory cytokine largely associated with the development of chronic inflammation. Notably, the adaptive immunity pathways were highlighted in IR7 and DR7, including the T-cell receptor signaling pathway, natural killer cell-mediated cytotoxicity, cell adhesion molecule pathway, and chemokine signaling pathway. This finding indicates that the inflammatory responses of replanted teeth may be highlighted in this phase. Moreover, this finding can provide insights into the current guidelines for replanted teeth. Previous literature recommends that pulp extirpation of avulsed teeth should be performed within 2 weeks of replantation [8].

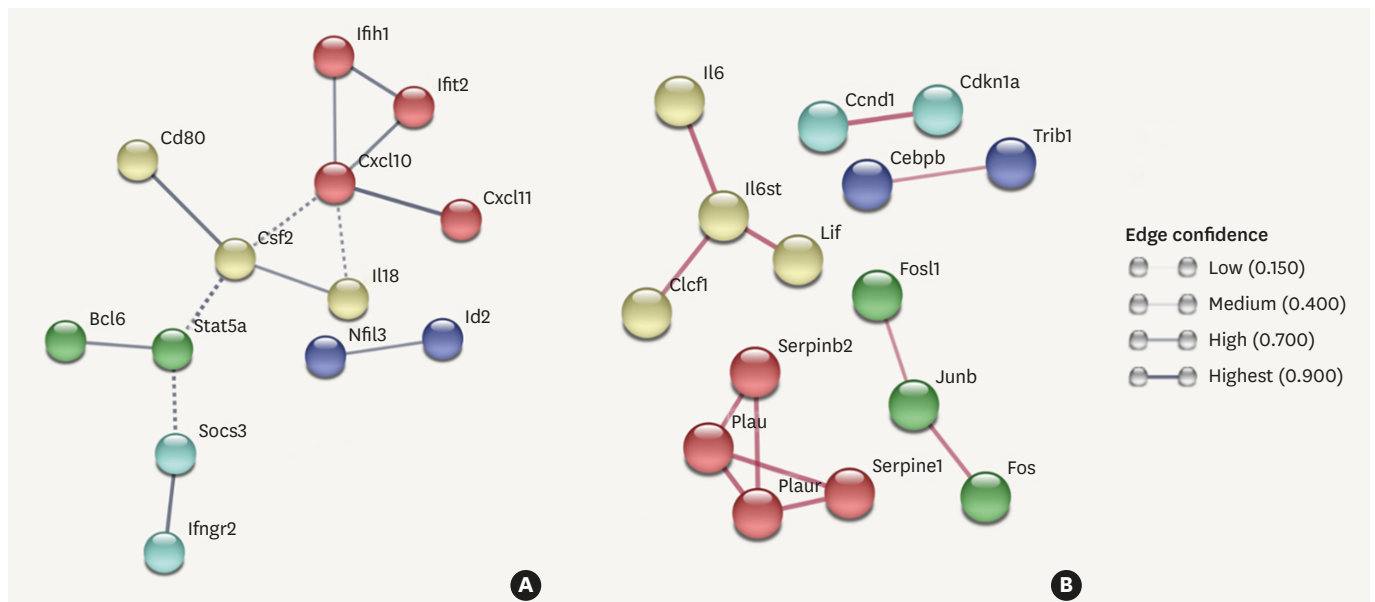


Figure 5. Protein-protein interaction network construction of core enriched genes in **Figure 4**. (A) Gene interaction networks significantly expressed in DR3. (B) Gene interaction networks significantly expressed in DR7. Unconnected nodes in the network are hidden. Colored nodes represent query proteins and the first shell of interactors. DR3: 3 days after delayed replantation, DR7: 7 days after delayed replantation.

Among the highly remarkable DEGs, the pattern of CXCL2 expression between IR and DR differed by time. CXCL2 expression was highly upregulated in both the IR and DR groups at 3 days. However, its expression was upregulated only at 7 days in DR. Upregulation of CXCL2 in DR was also confirmed in a previous study. The study reported marked expression of pro-inflammatory cytokines with increased storage duration [15]. This finding indicates that adverse events associated with bone pathology may be more likely to occur in cases of DR. CXCL2 directly mediates osteoclastogenesis [19]. A previous study revealed that CXCL2 blockage in lipopolysaccharide-treated bone marrow cells inhibits osteoclast recruitment and prevents bone destruction [20]. Moreover, there is evidence of a strong linkage between CXCL2 and the NF- κ B pathway [21].

Periodontal tissue destruction depends on the intensity and duration of the immune response. Dysregulation of the pro-inflammatory and anti-inflammatory cytokine balance may lead to bone and collagen destruction [22]. Thus, we performed a hallmark gene set enrichment analysis to investigate differences in DEGs between IR and DR over time. The enrichment results revealed that the identified DEGs in the DR group at 3 days were positively correlated with the oxidative phosphorylation pathway compared to the IR group. Reactive oxygen species (ROS), which are the byproducts of oxidative phosphorylation, have pivotal roles in various physiological processes. Accumulating evidence has demonstrated that an increased level of ROS resulting from oxidative phosphorylation is present during osteogenic differentiation of mesenchymal stem cells, including PDL stem cells [23]. However, overproduction of ROS can induce an inflammatory environment, and this dysregulation may result in periodontal destruction [24]. A previous study showed that ROS can induce IL-8 production in human PDL cells and demonstrated that ROS production in an inflammatory environment may expedite periodontal destruction [25]. This finding suggests that healing may be hindered in DR in this phase.

The enrichment results revealed that the identified DEGs in the DR condition at 3 days were positively correlated with TNF- α signaling via the NF- κ B pathway compared to IR. Periodontal tissues synthesize TNF- α and RANKL under pathological conditions [26]. TNF- α has a significant role in osteoclast differentiation and proliferation and is strongly linked to bone resorption in periodontal tissues [3]. TNF- α cannot induce osteoclastogenesis alone; it acts in concert with RANKL to induce osteoclastic differentiation via the NF- κ B pathway [27]. This result is consistent with the findings of an *in vivo* study that imitated a DR environment. The study showed that the TNF- α signaling pathway was highlighted as the hallmark gene set when human PDL cells were preserved in storage medium [15]. This finding suggests that osteoclast activity may be more upregulated in DR, thereby increasing the incidence of root resorption.

Among the core enriched DEGs of IR3 and DR3, CXCL10, CSF2, and STAT5A were identified from PPI network construction. Some evidence has demonstrated the relevance of CXCL10 in osteoclast activity, and CXCL10 was found to have a direct influence on the recruitment of osteoclast precursor cells [28]. In another study with a gene-knockout mouse model, CXCL10 accelerated RANKL-mediated osteoclastogenesis [29]. Moreover, increased CXCL10 concentrations in saliva and serum were confirmed in chronic periodontitis patients and these findings correlated with the severity of bone loss [30]. CSF2 is a cytokine produced by T cells, macrophages, and fibroblasts when immune stimuli are recognized. The presence of CSF2 is strongly related to TNF- α production. A previous study demonstrated that TNF- α with CSF2 influences the pathogenesis of chronic periodontitis and may increase inflammatory potential in periodontitis [31]. STAT5A participates in CSF2 expression [32]. Hence, STAT5A positively regulates TNF- α production via the JAK/STAT pathway [33].

Interestingly, the NES of TNF- α signaling via the NF- κ B pathway in DR reversed at 7 days compared to 3 days. The core enriched DEGs were differentially identified compared to the replanted teeth at 3 days. SERPINB2, FOS, JUNB, and IL-6 were identified from PPI network construction; the identified DEGs differentially regulated the pathogenesis of TNF- α signaling via the NF- κ B pathway. SERPINB2 is present in very high concentrations in the gingival fluid. It is an inhibitor of serine proteases, which are mainly produced by bacteria associated with periodontal inflammation [34]. However, there is some controversy regarding the role of SERPINB2 in periodontal disease. A previous clinical study showed that higher levels of SERPINB2 were associated with a less severe inflammatory reaction to periodontal pathogens [35]. An *in vivo* study showed that SERPINB2 was upregulated in the presence of periodontal inflammation [36]. The FOS family and JUN family, including JUNB, form AP-1 proteins and promote wound healing [37]. IL-6 upregulates RANKL expression in osteoblasts, resulting in the differentiation of osteoclasts [3].

Among the enrichment results of replanted teeth at 7 days, TGF- β signaling drew particular attention. TGF- β signaling was negatively correlated with DR compared to IR. TGF- β is a cytokine that participates in bone metabolism. TGF- β has the potential to promote PDL regeneration. In the periodontal inflammatory microenvironment, high TGF- β production by periodontal tissues promotes the differentiation and repair of periodontal fibroblasts. A previous study confirmed that TGF- β in human platelet-rich plasma (PRP) stimulated PDL cells and type I collagen synthesis in the PDL [38]. Another study showed more favorable periodontal healing in dog teeth replanted with PRP due to the continuous local release of various growth factors associated with wound healing and tissue repair [39]. Hence, TGF- β is highly expressed in the presence of upregulated IL-6 and modulates the resolution of inflammation [40]. Since these pathways present different functional characteristics, it may

be reasonable to assume that the net effect of their interactions is more important than the role of specific pathways.

The present study identified DEG profiles after tooth replantation. A significant finding was that the immune responses in periodontal tissues after replantation were mainly associated with TNF- α signaling via the NF- κ B pathway. However, the present study has several limitations. First, this specific topic with RNA-seq still needs more research in the field; hence, the current pilot study conveniently determined the sample size. Future studies will need to use more meticulous calculations to identify the sample size. Furthermore, since this study used palatal soft tissue biopsy samples, differences in regulatory mechanisms between the IR and DR conditions might not be ideally identified. Next, the prognosis of replanted teeth was not considered. Replanted teeth with the same extra-oral time may have different prognoses. Therefore, further gene expression studies in replanted teeth according to specific complications are necessary. Furthermore, in evaluating periodontal tissue destruction or the quality of replantation, a further study will need to incorporate additional assessments such as histologic analyses and radiographic evaluations for a more in-depth investigation. Finally, this study only included evaluation time points at 3 and 7 days, although considerable changes in DEG profiles can also occur after these phases. Gene expression analysis in replanted teeth with more extended periods will be needed in the future.

REFERENCES

1. Carnes DL, Maeder CL, Graves DT. Cells with osteoblastic phenotypes can be explanted from human gingiva and periodontal ligament. *J Periodontol* 1997;68:701-7.
[PUBMED](#) | [CROSSREF](#)
2. Hajishengallis G. Immunomicrobial pathogenesis of periodontitis: keystones, pathobionts, and host response. *Trends Immunol* 2014;35:3-11.
[PUBMED](#) | [CROSSREF](#)
3. Pan W, Wang Q, Chen Q. The cytokine network involved in the host immune response to periodontitis. *Int J Oral Sci* 2019;11:30.
[PUBMED](#) | [CROSSREF](#)
4. Yu CY, Abbott PV. Responses of the pulp, periradicular and soft tissues following trauma to the permanent teeth. *Aust Dent J* 2016;61 Suppl 1:39-58.
[PUBMED](#) | [CROSSREF](#)
5. Andreasen JO. Relationship between surface and inflammatory resorption and changes in the pulp after replantation of permanent incisors in monkeys. *J Endod* 1981;7:294-301.
[PUBMED](#) | [CROSSREF](#)
6. Andreasen JO, Borum MK, Jacobsen HL, Andreasen FM. Replantation of 400 avulsed permanent incisors. 4. Factors related to periodontal ligament healing. *Endod Dent Traumatol* 1995;11:76-89.
[PUBMED](#) | [CROSSREF](#)
7. Kinirons MJ, Gregg TA, Welbury RR, Cole BO. Variations in the presenting and treatment features in reimplanted permanent incisors in children and their effect on the prevalence of root resorption. *Br Dent J* 2000;189:263-6.
[PUBMED](#) | [CROSSREF](#)
8. Andersson L, Andreasen JO, Day P, Heithersay G, Trope M, Diangelis AJ, et al. International Association of Dental Traumatology guidelines for the management of traumatic dental injuries: 2. Avulsion of permanent teeth. *Dent Traumatol* 2012;28:88-96.
[PUBMED](#) | [CROSSREF](#)
9. Ahn HJ, Nam OH, Lee HS, Kim EC, Cohenca N, Choi SC. Expression of inflammatory cytokines and MMPs on replanted teeth at different extra-alveolar time: an *ex vivo* and *in vivo* study. *Int J Paediatr Dent* 2016;26:301-9.
[PUBMED](#) | [CROSSREF](#)

10. Panzarini SR, Okamoto R, Poi WR, Sonoda CK, Pedrini D, da Silva PE, et al. Histological and immunohistochemical analyses of the chronology of healing process after immediate tooth replantation in incisor rat teeth. *Dent Traumatol* 2013;29:15-22.
[PUBMED](#) | [CROSSREF](#)
11. Taiete T, Casarin RC, Ruiz KG, Nociti FH Jr, Sallum EA, Casati MZ. Transcriptome of healthy gingival tissue from edentulous sites in patients with a history of generalized aggressive periodontitis. *J Periodontol* 2018;89:93-104.
[PUBMED](#)
12. Jeon YS, Cha JK, Choi SH, Lee JH, Lee JS. Transcriptomic profiles and their correlations in saliva and gingival tissue biopsy samples from periodontitis and healthy patients. *J Periodontal Implant Sci* 2020;50:313-26.
[PUBMED](#) | [CROSSREF](#)
13. Wang Z, Gerstein M, Snyder M. RNA-Seq: a revolutionary tool for transcriptomics. *Nat Rev Genet* 2009;10:57-63.
[PUBMED](#) | [CROSSREF](#)
14. Nam OH, Kim JH, Choi SC, Kim Y. Time-dependent response of human deciduous tooth-derived dental pulp cells treated with TheraCal LC: functional analysis of gene interactions compared to MTA. *J Clin Med* 2020;9:531.
[PUBMED](#) | [CROSSREF](#)
15. Nam OH, Oh TJ, Lee JH, Hwang YS, Choi SC. Differential gene expression profiles of human periodontal ligament cells preserved in Hank's balanced salt solution and milk. *Dent Traumatol* 2020;36:58-68.
[PUBMED](#) | [CROSSREF](#)
16. Quinlan AR, Hall IM. BEDTools: a flexible suite of utilities for comparing genomic features. *Bioinformatics* 2010;26:841-2.
[PUBMED](#) | [CROSSREF](#)
17. Iwasaki A, Medzhitov R. Toll-like receptor control of the adaptive immune responses. *Nat Immunol* 2004;5:987-95.
[PUBMED](#) | [CROSSREF](#)
18. Lee C, Lim HK, Sakong J, Lee YS, Kim JR, Baek SH. Janus kinase-signal transducer and activator of transcription mediates phosphatidic acid-induced interleukin (IL)-1 β and IL-6 production. *Mol Pharmacol* 2006;69:1041-7.
[PUBMED](#) | [CROSSREF](#)
19. Ha J, Lee Y, Kim HH. CXCL2 mediates lipopolysaccharide-induced osteoclastogenesis in RANKL-primed precursors. *Cytokine* 2011;55:48-55.
[PUBMED](#) | [CROSSREF](#)
20. Valerio MS, Herbert BA, Basilakos DS, Browne C, Yu H, Kirkwood KL. Critical role of MKP-1 in lipopolysaccharide-induced osteoclast formation through CXCL1 and CXCL2. *Cytokine* 2015;71:71-80.
[PUBMED](#) | [CROSSREF](#)
21. De Plaen IG, Han XB, Liu X, Hsueh W, Ghosh S, May MJ. Lipopolysaccharide induces CXCL2/macrophage inflammatory protein-2 gene expression in enterocytes via NF- κ B activation: independence from endogenous TNF- α and platelet-activating factor. *Immunology* 2006;118:153-63.
[PUBMED](#) | [CROSSREF](#)
22. Morand DN, Davideau JL, Clauss F, Jessel N, Tenenbaum H, Huck O. Cytokines during periodontal wound healing: potential application for new therapeutic approach. *Oral Dis* 2017;23:300-11.
[PUBMED](#) | [CROSSREF](#)
23. Li Q, Gao Z, Chen Y, Guan MX. The role of mitochondria in osteogenic, adipogenic and chondrogenic differentiation of mesenchymal stem cells. *Protein Cell* 2017;8:439-45.
[PUBMED](#) | [CROSSREF](#)
24. Chapple IL, Matthews JB. The role of reactive oxygen and antioxidant species in periodontal tissue destruction. *Periodontol* 2000 2007;43:160-232.
[PUBMED](#) | [CROSSREF](#)
25. Lee YS, Bak EJ, Kim M, Park W, Seo JT, Yoo YJ. Induction of IL-8 in periodontal ligament cells by H(2)O (2). *J Microbiol* 2008;46:579-84.
[PUBMED](#) | [CROSSREF](#)
26. Ogasawara T, Yoshimine Y, Kiyoshima T, Kobayashi I, Matsuo K, Akamine A, et al. In situ expression of RANKL, RANK, osteoprotegerin and cytokines in osteoclasts of rat periodontal tissue. *J Periodontal Res* 2004;39:42-9.
[PUBMED](#) | [CROSSREF](#)
27. Luo G, Li F, Li X, Wang ZG, Zhang B. TNF- α and RANKL promote osteoclastogenesis by upregulating RANK via the NF- κ B pathway. *Mol Med Rep* 2018;17:6605-11.
[PUBMED](#) | [CROSSREF](#)

28. Sucur A, Jajic Z, Artukovic M, Matijasevic MI, Anic B, Flegar D, et al. Chemokine signals are crucial for enhanced homing and differentiation of circulating osteoclast progenitor cells. *Arthritis Res Ther* 2017;19:142.
[PUBMED](#) | [CROSSREF](#)
29. Yim HY, Park C, Lee YD, Arimoto K, Jeon R, Baek SH, et al. Elevated response to type I IFN enhances RANKL-mediated osteoclastogenesis in Usp18-knockout mice. *J Immunol* 2016;196:3887-95.
[PUBMED](#) | [CROSSREF](#)
30. Aldahlawi S, Youssef AR, Shahabuddin S. Evaluation of chemokine CXCL10 in human gingival crevicular fluid, saliva, and serum as periodontitis biomarker. *J Inflamm Res* 2018;11:389-96.
[PUBMED](#) | [CROSSREF](#)
31. Gamonal J, Sanz M, O'Connor A, Acevedo A, Suarez I, Sanz A, et al. Delayed neutrophil apoptosis in chronic periodontitis patients. *J Clin Periodontol* 2003;30:616-23.
[PUBMED](#) | [CROSSREF](#)
32. Feldman GM, Rosenthal LA, Liu X, Hayes MP, Wynshaw-Boris A, Leonard WJ, et al. STAT5A-deficient mice demonstrate a defect in granulocyte-macrophage colony-stimulating factor-induced proliferation and gene expression. *Blood* 1997;90:1768-76.
[PUBMED](#) | [CROSSREF](#)
33. Garcia de Aquino S, Manzolli Leite FR, Stach-Machado DR, Francisco da Silva JA, Spolidorio LC, Rossa C Jr. Signaling pathways associated with the expression of inflammatory mediators activated during the course of two models of experimental periodontitis. *Life Sci* 2009;84:745-54.
[PUBMED](#) | [CROSSREF](#)
34. Neilands J, Bikker FJ, Kinnby B. PAI-2/SerpinB2 inhibits proteolytic activity in a P. gingivalis-dominated multispecies bacterial consortium. *Arch Oral Biol* 2016;70:1-8.
[PUBMED](#) | [CROSSREF](#)
35. Kinnby B. The plasminogen activating system in periodontal health and disease. *Biol Chem* 2002;383:85-92.
[PUBMED](#) | [CROSSREF](#)
36. Yamamoto E, Awano S, Koseki T, Ansai T, Takehara T. Expression of endothelin-1 in gingival epithelial cells. *J Periodontal Res* 2003;38:417-21.
[PUBMED](#) | [CROSSREF](#)
37. Beikler T, Peters U, Prior K, Eisenacher M, Flemmig TF. Gene expression in periodontal tissues following treatment. *BMC Med Genomics* 2008;1:30.
[PUBMED](#) | [CROSSREF](#)
38. Okuda K, Kawase T, Momose M, Murata M, Saito Y, Suzuki H, et al. Platelet-rich plasma contains high levels of platelet-derived growth factor and transforming growth factor-beta and modulates the proliferation of periodontally related cells *in vitro*. *J Periodontol* 2003;74:849-57.
[PUBMED](#) | [CROSSREF](#)
39. Zhao YH, Zhang M, Liu NX, Lv X, Zhang J, Chen FM, et al. The combined use of cell sheet fragments of periodontal ligament stem cells and platelet-rich fibrin granules for avulsed tooth reimplantation. *Biomaterials* 2013;34:5506-20.
[PUBMED](#) | [CROSSREF](#)
40. Morandini AC, Sipert CR, Ramos-Junior ES, Brozoski DT, Santos CF. Periodontal ligament and gingival fibroblasts participate in the production of TGF- β ², interleukin (IL)-8 and IL-10. *Braz Oral Res* 2011;25:157-62.
[PUBMED](#) | [CROSSREF](#)